FREE-BREATHING FAT-WATER-SEPARATED LIVER MRI USING A MULTI-ECHO 3D STACK-OF-STARS TECHNIQUE

Tess Armstrong[1,2], Isabel Dregely[1], Fei Han[1], Ziwu Zhou[1], Kyung Sung[1,2], Peng Hu[1,2], and Holden Wu[1,2]

[1]*Radiological Sciences, University of California Los Angeles, Los Angeles, CA, United States,* [2]*Biomedical Physics, University of California Los Angeles, Los Angeles, CA, United States*

Introduction: Non-alcoholic fatty liver disease (NAFLD) affects about 20-30% of the general population and is the leading cause of chronic liver disease in the United States.[1–3] The gold standard for diagnosis and monitoring is by an invasive biopsy to characterize fatty infiltration in the liver, however biopsy has associated morbidity and suffers from spatial sampling bias.[1–3] Alternatively, MRI methods based on multi-echo fat-water separation can provide non-invasive 3D characterization of fat in the entire liver.[4–6] However, current multi-echo MRI methods based on Cartesian sampling are susceptible to respiratory motion-induced coherent aliasing artifacts and therefore the scan is routinely limited to a single breath hold (BH). The limited scan time of BH acquisitions makes it challenging to achieve volumetric coverage, high spatial resolution, desirable echo times, and artifact-free images for liver fat-water separation. In addition, BH may even be impossible for certain patients. Compared to Cartesian MRI, non-Cartesian MRI provides robustness to motion and can support high degrees of acceleration.[7] In this work, we developed a new multi-echo MRI technique based on the **3D stack-of-stars** trajectory to enable **free-breathing (FB) fat-water-separated imaging of the liver**. The feasibility of this technique and quality of fat-water separation is compared to a 3D Cartesian BH technique in healthy volunteers.

Methods: [*Sequence Design*] An RF-spoiled gradient echo sequence using the golden-angle-ordered (θ_G) 3D stack-of-stars trajectory was implemented (**Fig. 1a**). All radial readouts at the same angle were acquired along k_z before moving on to the next angle. For the first version, bipolar multi-echo readouts covering the entire set of TEs were acquired every TR ("single TR", **Fig. 1b**). To achieve smaller echo spacing, a second version acquired multiple echoes interleaved across two TRs and alternated between the two as the radial angle progressed ("interleaved TR", **Fig. 1c**). Note that this creates two-fold *k*-space undersampling vs. the single-TR version when the number of TRs is constant. [*Experiments*] 3D liver images were acquired in three healthy volunteers on a 3T scanner (Skyra, Siemens) using 1) a 6-echo 3D stack-of-stars single TR FB sequence, 2) a 6-echo 3D stack-of-stars interleaved TR FB sequence with 3 echoes per TR, and 3) a 6-echo 3D Cartesian BH sequence.[8] Typical imaging parameters are listed in **Table 1**. A 32-channel body array coil was used for all acquisitions. [*Reconstruction*] For the 3D stack-of-stars acquisitions, gridding was performed first, followed by fat-water separation using a graph cut algorithm with a 6-peak fat model and a single effective R2* for each voxel.[9] Fat and water images from the 3D Cartesian acquisitions were calculated by scanner software using a similar signal model.[8] [*Assessment*] Fat and water images were viewed in 3D software (OsiriX) to assess separation quality.

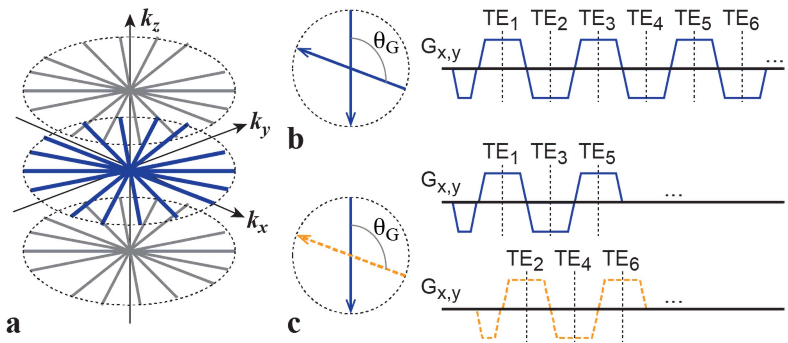

Fig 1: a) 3D stack-of-stars *k*-space trajectory. b) Radial readouts are rotated continually by the golden angle (θ_G) and multiple echoes are acquired every TR ("single TR"). c) The multiple echoes are interleaved across two TRs and the TRs are alternately acquired as the radial readout angle is rotated by θ_G ("interleaved TR").

Imaging Parameters	Cartesian	Single TR	Interleaved TR
TR (ms)	8.85	8.85	5.7
TE (ms)	1.23, 2.46, 3.69, 4.92, 6.15, 7.38	1.23, 2.46, 3.69, 4.92, 6.15, 7.38	1.23, 1.84, 2.45, 3.06, 3.67, 4.28
Delta TE (ms)	1.23	1.23	0.61
Matrix	256 x 256 x 48	256 x 256 x 48	256 x 256 x 48
FOV (mm x mm x mm)	420 x 420 x 144	420 x 420 x 144	420 x 420 x 144
Radial spokes	N/A	804	1024
Flip Angle (degrees)	5	5	5
Bandwidth (Hz/pixel)	1030	1028	1028
Parallel Imaging	4-fold	N/A	N/A
Scan Time (min:sec)	0:17 (BH)	6:38 (FB)	5:19 (FB)

Table 1: The typical imaging parameters for the 3D stack-of-stars (interleaved and single TR) FB and Cartesian BH scans.

Results: Representative liver fat and water images from similar slices are shown in **Fig 2**. The slices from BH and FB scans could not be perfectly matched due to differences in the respiratory position. Fat-water separation quality using the FB 3D stack-of-stars and BH Cartesian acquisitions were in good agreement. Minor radial streaking artifacts were visible in certain slices of the 3D stack-of-stars images due to motion and k-space undersampling, but no coherent aliasing artifacts were observed. In this example (Fig. 2), Cartesian BH images appeared noisier than the 3D stack-of-stars FB images.

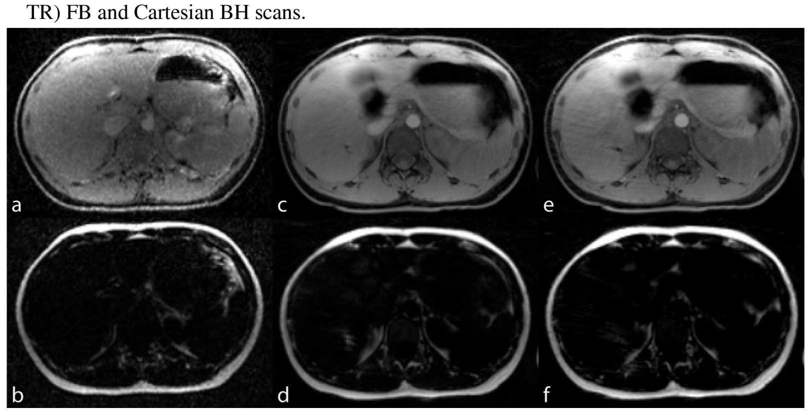

Fig 2: The water (a, c and e) fat (b, d and f) images for the BH Cartesian (a-b), the single TR (c-d) and the interleaved TR (e-f) stack-of-stars FB scans for the same volunteer.

Discussion and Conclusion: The proposed multi-echo 3D stack-of-stars technique was able to obtain FB fat-water-separated images of the liver without coherent motion artifacts. The overall quality of fat-water separation was comparable to a BH Cartesian technique. Currently, the number of radial spokes is oversampled to average out motion effects. Extensions of our technique to incorporate self-navigated motion compensation and non-Cartesian parallel imaging can suppress streaking artifacts and reduce scan time. With further development, the presented multi-echo 3D stack-of-stars technique has potential to enable free-breathing characterization of liver fat.

References: [1] Bellentani et al., Ann. Hepatol. 2009; S4–8. [2] De Alwis et al., *J. Hepatol.* 2008; 48. [3] Vernon et al., *Aliment. Pharmacol. Ther.* 2011; 34: 274–285. [4] Yu et al., JMRI 2007; 26: 1153–61. [5] Liu et al. MRM 2007; 58: 354–364. [6] Ma et al., JMRI 2008; 28: 543–58. [7] Glover et al., MRM 1992; 28: 275–289. [8] Zhong et al., MRM 2014; 72:1353-1365. [9] Hernando et al., MRM 2010; 63: 79–90.